J. Automation & Systems Engineering 7-4 (2013): 125-142

Journal of Automation & Systems Engineering

Regular paper

Application of Extended Observer with Gain Scheduling Control to Internal Combustion Engine Model

Simon Omekanda and Dr. Mohamed A. Zohdy

Abstract- In this paper, an extended observer was investigated and then implemented for generating approximate state feedback for an Internal Combustion (IC) engine. IC engines are inherently highly nonlinear in nature, therefore, present a problem for system modeling and observer design. A state-dependent gain scheduling control was used to improve state estimation. An extended observer was implemented for providing state feedback of the IC model presented in this paper. The extended observer's performance was analyzed by looking at the output response to a desired output command, added model disturbance and initial condition variation. Moreover, the robustness of the closed loop system to parameter variations was tested. Matlab was used for simulation and the results shown in this paper demonstrated that the extended observer was a good tool for IC engine control. The use of state-dependent gain scheduling allowed the extended observer to stay robust for the entire operating range and showed good results to meeting a desired output command.

Keywords: Extended observer, Gain scheduling, Engine control.

1. INTRODUCTION

Modern automotive IC engines have undergone many modifications and improvements in recent years with respect to size, efficiency and power. This is due to economical and environmental concerns as well as growing stringent government regulations. Engine dynamical modeling has, therefore, become very important in order to understand the performance advantages. There are two main foci for modeling: control and state feedback estimation. Vast studies and applications pertaining to system control and state estimation exist in literature [1-7]. Because observers are inherently model-based, they tend to deal well with system errors and fluctuations and can even be used in the case of uncertain systems [8] The drawback is that common state observers are only derived for linear systems [9-11]. They have been used based on simulation for many practical engineering applications and have shown to be both reliable and efficient [12-16]. While nonlinear observers have been used on specific application and subsystems of the engine as in [16 17], we demonstrate its ability to estimate the states of a multivariable model. The advantage of a nonlinear estimator, such as the extended observer, is significant in comparison to a linear observer. Linear observers are designed based on models that were previously already linearized, therefore already include a certain degree of error.

Simon Omekanda Electrical and Computer Engineering Department, Oakland University, Rochester, Michigan, USA Email: simon.omekanda@ieee.edu, zohdyma@oakland.edu

Using a nonlinear estimator takes away this burden and any nonlinear system can be applied.

A state-dependent gain schedule was created for the observer. This was done to ensure observer robustness and stability for the entire operating range of the system. Gain scheduling control is one of the most popular nonlinear control methods and has been used throughout many fields such as aerospace, automotive and process control [18]. We want to demonstrate that an extended observer, along with a state-dependent gain scheduling scheme, can be utilized and implemented to accurately estimate the states of an IC engine model. Furthermore, we designed a closed loop control system to meet a desired output command and test the robustness and performance to an increase to the model disturbance, a variation in the initial conditions and model parameters. Simulations of the results were performed in Matlab.

2. INTERNAL COMBUSTION ENGINE MODEL

A linear time-varying state space can be expressed by the following equations:

$$\dot{x} = A(t) * x(t) + B(t) * u(t),$$
$$y = C(t) * x(t) + D(t) * u(t), \qquad (1)$$

where k is the sampling time, u is the system input, A, B, C and D are respectively constant state, input, output and feedthrough matrices of size $n\,x\,n$, $m\,x\,m$, $p\,x\,n$, and $p\,x\,m$ respectively. n is the number of states in the system, m is the number of inputs, p is the number of outputs and x is the state vector. In this paper, a class of nonlinear observers was designed for use in the time-varying nonlinear system of the form:

$$\dot{x} = \tilde{f}(x(t), u(t)) \qquad (2)$$

where $\tilde{f}$ denotes a nonlinear function. Such nonlinear systems are used to describe internal combustion engines. Internal combustion engines are multivariable models which describe the dynamical behavior of the engine. The model is comprised of mathematical equations modeling the change in various states of the engine. Fig. 1 displays a block diagram of the subsystems of an IC model. In this paper, we used an existing model proposed by Powell in which he laid out the state equations for different subsystems of a V8 (6.6L) Ford engine [19]. For simplicity, only 4 states were used $x = \left[x_1\ x_2\ x_3\ x_4\right]^T$ in which x_i are respectively: Intake mass air flow ($\dot{M}_i$), mass air flow into the cylinders ($\dot{M}_o$), manifold pressure (P_m) and engine speed (N). The system input, u , is the throttle angle which starts the air intake process. We have discussed each nonlinear state equation in the next 4 sections. The parameters used are provided in Table 1.

Table 1: Nomenclature

M_i	Intake Mass Flow (lb)
θ	Throttle Angle (radians)
P_m	Manifold Pressure (psi)
N	Engine Speed (RPM)
$\dot{M}_o$	Mass Air Flow into cylinders (lb)
$\dot{M}_e$	Exhaust Gas recirculation Flow Rate (lb/hr)
T_{eng}	Engine Torque (ft-lb)
T_{load}	Load Torque (ft-lb)
T_e	Engine inertia (ft-lb-sec^2/radians)
P_a	Ambient Pressure (psi)

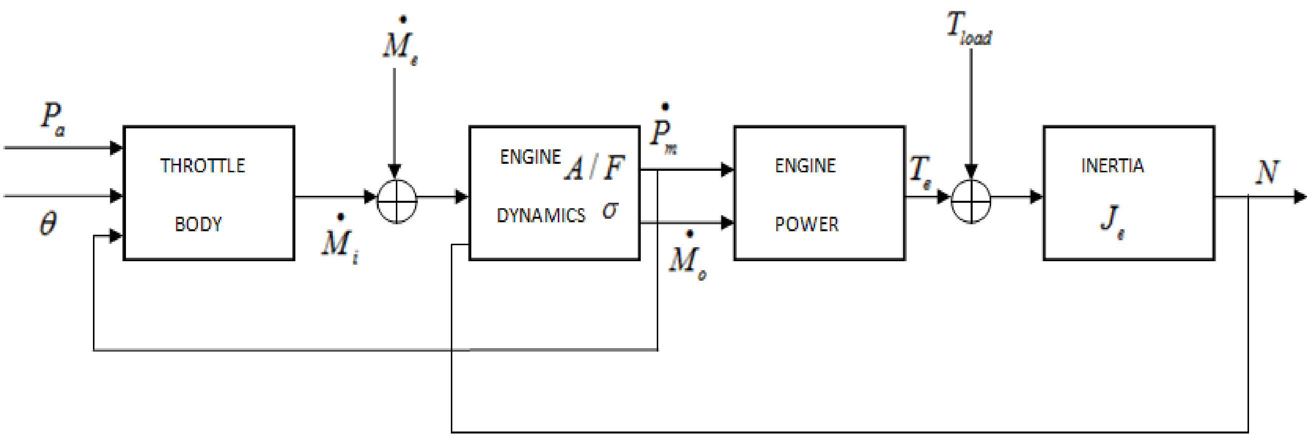

Figure 1: Model of Internal Combustion Engine

2.1 INTAKE MASS AIR FLOW

It is very important to have a precise estimation of the intake mass air flow in order to have optimal mixing with the fuel to meet torque demand, while increasing fuel and power efficiency. The system input is the throttle plate angle which has a range which varies on the particular engine, but usually has a minimum angle of 7° to 12° to prevent air restriction. The intake mass air flow depends on the manifold pressure, the ambient pressure and the throttle plate angle, which lets the air come into the intake manifold. The pressure in the manifold is lower than the ambient pressure, creating a vacuum which sucks the air in to be mixed with fuel. There are two different type of flows: sonic and subsonic. A sonic flow occurs when the change in pressure $\Delta P = P_m - P_a$, is equal or greater than half of the ambient pressure. In that case, the intake mass air flow, $\dot{M}_i$, is only dependent on the throttle angle. Nonetheless, because a sonic flow tends to only have an effect at idle speeds and transients rather than steady state conditions, on which the parameters for this model were calculated, a subsonic flow is assumed. The equation for the subsonic flow is as follows:

$$\dot{M}_i = 0.96(\theta^2 - 25) * \sqrt{\left(\frac{P_m}{P_a} - \frac{P_m^{\ 2}}{P_a}\right)} \tag{3}$$

where $\dot{M}_i$ is the intake mass air flow rate in pounds per hour.

2.2 MASS AIR FLOW INTO CYLINDER

after the air has passed through the throttle orifice and has been mixed with the fuel, it is injected into the cylinders for combustion. As a means of control, it is good to know how fast the air is injected into the cylinders for optimal combustion. With the advance in electronic systems, intake valve opening and closing can be controlled quite easily and precisely. Therefore, by being able to estimate the flow rate of the air into the engine, calculations can be made to make sure that the desired amount of mixture is present in the cylinders at a certain time to meet torque demands. The non-linear equation is a function of the manifold pressure and engine speed. This nonlinear relationship is referred to as the speed-density mass flow:

$$\dot{M}_o = 0.09125 * N * P_m - 0.0006875 * N * P_m^{\ 2} \tag{4}$$

where $\dot{M}_o$ is the mass air flow rate into cylinders in pounds per hour.

2.3 MANIFOLD PRESSURE

Manifold pressure is an important state because together with the manifold volume and temperature, it is used to calculate the density inside the manifold. The density is key in mixing because the higher the density, the better air mixes with fuel to attain optimal combustion results. In an IC engine, the temperature is kept low by the cooling system. The pressure is controlled in order to create a greater vacuum, as well as to stay within a certain range for the density to be kept at a desired value for mixing. All these factors are dependent on the torque and speed demands. The relationship between density (ρ), pressure (P) and temperature (T) is demonstrated in *the Ideal Gas Law* $\rho = \frac{PV}{RT}$ where R is the universal gas constant. All this information is calculated by the Electronic Control Unit (ECU) to meet torque demand and desired engine speed (RPM). The model also includes the effect of the Exhaust Gas Recirculation (EGR). It models the change in pressure as the difference in the gases present in the manifold and the gases that are inserted into the cylinders:

$$\dot{P}_m = K_p\,(\dot{M}_i + \dot{M}_e - \dot{M}_o) \quad (5)$$

where K_p is the proportionality constant .It is a function of the Universal Gas Constant, specific heat parameters, manifold temperature and the manifold volume. The exhaust gas recirculation flow rate, $\dot{M}_e$, was kept as a constant for simplification of the system. Both K_p and $\dot{M}_e$ were chosen based on results given in Powell's paper [9]. Equation (5) can be re-written in terms of the system input, manifold pressure and engine speed as follows:

$$\dot{P}_m = K_p[(0.96\theta^2 - 24)\sqrt{\frac{P_m}{P_a} - \frac{P_m}{P_a}^2} - 0.09125 * N * P_m - 0.0006875 * N * P_m{}^2 + \dot{M}_e \quad (6)$$

2.4 ENGINE SPEED

As the pistons rotate the crankshaft and the torque demand changes, they experience a positive or negative acceleration (deceleration) which, as seen in the equation below, is affected by the load torque and the inertia of the engine. This angular acceleration or deceleration is an important state to monitor, as it tells a lot about the output of the combustion which took place:

$$\dot{N} = \frac{30}{J_e \pi}(T_{eng} - T_{load}) \quad (7)$$

where J_e is the engine inertia. Since the engine torque depends on the engine speed (N), the mass flow into the cylinder ($\dot{M}_o$), the ignition angle (σ) and the air to fuel ratio (A/F), equation (7) can be re-written as follows:

$$\dot{N} = \frac{30}{J_e \pi}(-115 + 0.008NP_m + 0.0003NP_m{}^2 + 22A/F - 0.82A/F^2 + 0.927\sigma$$
$$-0.0227\sigma^2 + 0.00092\sigma N - 0.0179N - 0.000029N^2 - T_{load}) \quad (8)$$

For simplicity in the calculations, the ignition angle, σ , and the air to fuel ratio, A/F , were held constant.

3. EXTENDED OBSERVER

State observers are model-based tools that can estimate the internal states of a system such as given in equation 1. This assumes that the system observed is fully observable, often depicted $O \sim (A, C)$ [9, 10]. However, this applies only to linear systems. Since internal combustion engines are nonlinear systems, we need to use an extended observer to be able to estimate its states. Similarly to the linear observer, the system in equation 2 needs to be observable in order for the design of an extended observer to estimate its internal states [20]. The extended observer's design is based off the first order linearization of the nonlinear system in equation 2. We outlined the design of an extended observer for time varying nonlinear systems. The first step is the linearization of the system to be observed:

$$\dot{x} = J_{\tilde{f}}(x(t))|_{\bar{x}_i}\, x(t) + B(t)u(t) + g_{\bar{x}_i}(t) \tag{9}$$

where $\bar{x}_i$ are the operating conditions, which are an estimate of the state at time t.

The system Jacobian is denoted:

$$J_{\tilde{f}}(x(t))|_{\bar{x}_i} = \left. \begin{pmatrix} \frac{\partial \tilde{f}_1}{\partial x_1} & \cdots & \frac{\partial \tilde{f}_1}{\partial x_n} \\ \vdots & \ddots & \vdots \\ \frac{\partial \tilde{f}_n}{\partial x_1} & \cdots & \frac{\partial \tilde{f}_n}{\partial x_n} \end{pmatrix} \right|_{\bar{x}_{i=1\ldots n}} \tag{10}$$

And the vector of the collected deviations is described as:

$$g_{\bar{x}_i}(t) = \tilde{f}(\bar{x}_i(t)) - J_{\tilde{f}}(x(t))|_{\bar{x}_i} \tag{11}$$

Once the system is linearized, the next step is to design an observer in order to estimate its states. The extended observer has a similar form as the linear time invariant observer presented by Luenberger in [9]. The extended observer is represented as:

$$\dot{\hat{x}}(t)=A_{\hat{x}}(t)\hat{x}(t)+B(t)u(t)+K_{\hat{x}}(t)(y(t)-C\hat{x}(t))+g_{\hat{x}}(t) \tag{12}$$

$$y(t)=C\,x(t) \tag{13}$$

where $\hat{A}_{\hat{x}}(t)$ is the estimate of the state vector at time t and depends on the observed state $\hat{x}(t)$. $K_{\hat{x}}(t)$ is the gain matrix which depends on past estimates of $\hat{x}(t)$ and can be found using the pole placement method, which places poles at a desired location so that the error dynamics are driven to zero asymptotically [8]. The system in equation 1 has poles given by $|sI - A(t)| = 0$. A substitution of the state feedback law $u(t) = -K_{\hat{x}}(t)\hat{x}(t)$ into equation 1 places the roots of the full state feedback system at $\left|sI - (A(t) - B(t)K_{\hat{x}}(t)\right|$. $K_{\hat{x}}(t)$ can then be chosen to dictate the poles of the observer to be at a desired location which drives the observer estimate towards the system states. $g_{\hat{x}}(t)$ depends now on the estimate $\hat{x}(t)$, and is defined as:

$$g_{\hat{x}}(t)=\tilde{f}(\hat{x}(t))-J_{\tilde{f}}(\hat{x}(t))\,|_{\bar{x}_i} \tag{14}$$

4. STATE-DEPENDENT GAIN SCHEDULE

Due to most systems' nonlinearities, it is not always practical to use one controller but rather a group of controllers which adapt with the system changes to ensure stability. A great deal of research utilizing the gain scheduling approach, pertaining to the control of various types of engines, has been published [21-25]. In this paper, a gain schedule which depends on the current range of operation of the system's states was created. In doing this, the observer stability and robustness throughout the entire system operation was guaranteed. The following was done by changing the operating conditions, $\bar{x}_i$, in equation 10 depending on the range of the system's states and their rate of change. Changing the operating conditions will in turn also change the gain of the extended observer $K_{\hat{x}}(t)$. Fig. 2 shows the scheme used to build a more robust extended observer. This scheme could compute the gain in real-time by the Electronic Control Unit (ECU) and adjust the controller

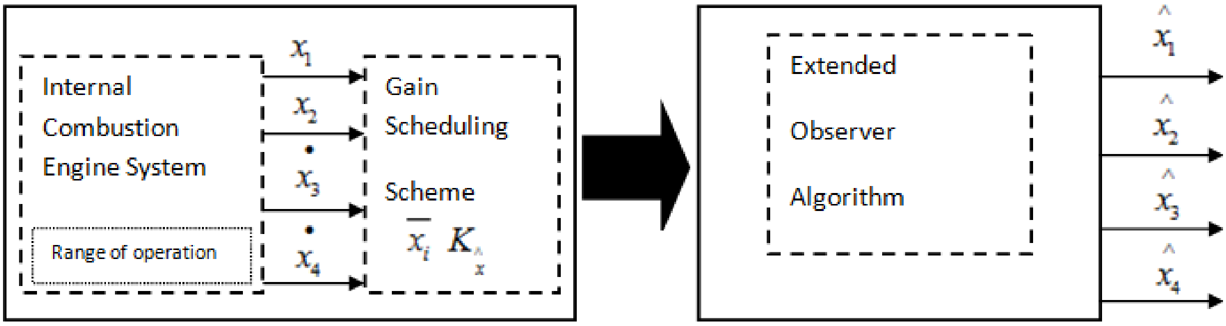

Figure 2: Gain Scheduling Scheme Block Diagram

The extended observer gain vector is dependent on the linearized state matrix. Therefore, each nonlinear equation, given in equations (3-5) and equation (8), were tested at different operating conditions to see how it affected the estimation. The operating conditions were chosen based on analysis of the detailed results of this particular engine model described in [19]. A set of 3 different operating conditions was chosen for each nonlinear equation and each combination was tested. Since each nonlinear equation depends on 2 different states, there were 9 combinations tested for each as shown in Figures 3 (a-d). It can be seen in each figure that certain operating conditions do not linearize the nonlinear equations adequately for the entire operating range. This could lead to stability problems as well as unreliability in the extended observer estimates. This is further evidence of the importance of a scheme such as the one developed in this paper. Table 2 displays all the operating conditions tested. These simulations results were used to choose the operating conditions which best linearized the system and the corresponding range of the state or the range of the rate-of-change of the state. A range was chosen for $\dot{M}_i$, $\dot{M}_o$, $\dot{P}$ and $\dot{N}$ which correspond to x_1, x_2, $\dot{x}_3$, and $\dot{x}_4$ respectively. It was more critical to monitor the rate of change in the speed and the manifold pressure, because by themselves they don't speak much of the immediate engine demands in real life conditions.

Table 2: Operating conditions tested

$\dot{M}_i$	$\dot{M}_o$	$\dot{P}_m$	$\dot{N}$
$\overline{\theta}_1 = 22^\circ$	$\overline{N}_1 = 900\,rpm$	$\overline{M}_{i1} = 500\,lb/hr$	$\overline{N}_1 = 900\,rpm$
$\overline{\theta}_2 = 42^\circ$	$\overline{N}_2 = 2000\,rpm$	$\overline{M}_{i2} = 1500\,lb/hr$	$\overline{N}_2 = 2000\,rpm$
$\overline{\theta}_3 = 72^\circ$	$\overline{N}_3 = 3600\,rpm$	$\overline{M}_{i3} = 2070\,lb/hr$	$\overline{N}_3 = 3600\,rpm$
$\overline{P}_m = 7.3\,psi$	$\overline{P}_{m1} = 7.6\,psi$	$\overline{M}_{o1} = 500\,lb/hr$	$\overline{P}_{m1} = 7.6\,psi$
$\overline{P}_m = 10\,psi$	$\overline{P}_{m2} = 10\,psi$	$\overline{M}_{o2} = 1000\,lb/hr$	$\overline{P}_{m2} = 10\,psi$
$\overline{P}_m = 14.6\,psi$	$\overline{P}_{m3} = 14.6\,psi$	$\overline{M}_{o3} = 1555\,lb/hr$	$\overline{P}_{m3} = 14.6\,psi$

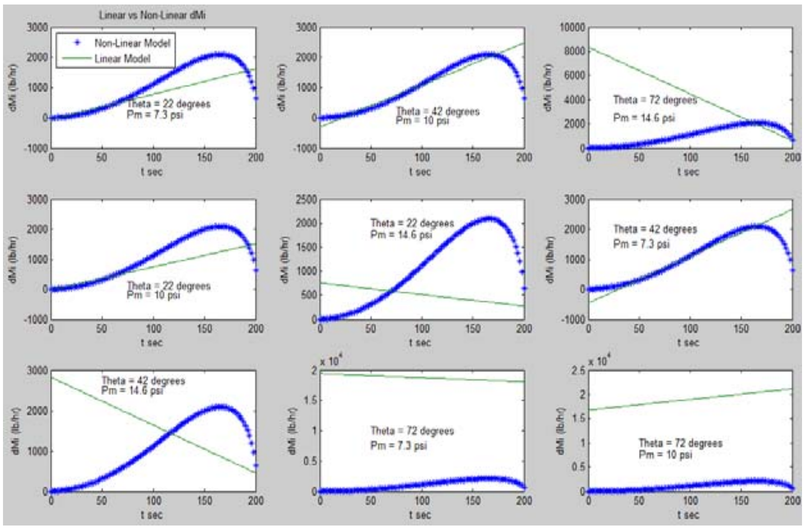
Linear vs Non-Linear dMi
Non-Linear Model
Linear Model
Theta = 22 degrees Pm = 7.3 psi
Theta = 42 degrees Pm = 10 psi
Theta = 72 degrees Pm = 14.6 psi
Theta = 22 degrees Pm = 10 psi
Theta = 22 degrees Pm = 14.6 psi
Theta = 42 degrees Pm = 7.3 psi
Theta = 42 degrees Pm = 14.6 psi
Theta = 72 degrees Pm = 7.3 psi
Theta = 72 degrees Pm = 10 psi
dMi (lb/hr)
t sec

(a)

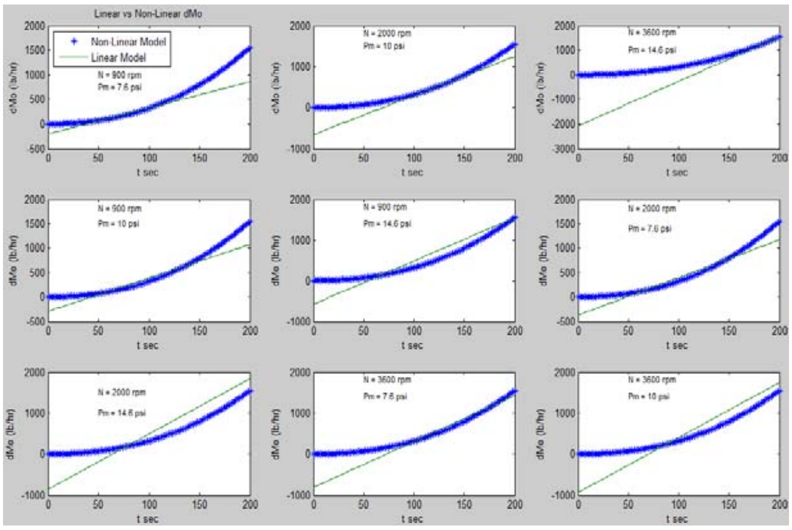
Linear vs Non-Linear dMo
Non-Linear Model
Linear Model
dMo (lb/hr)
t sec

(b)

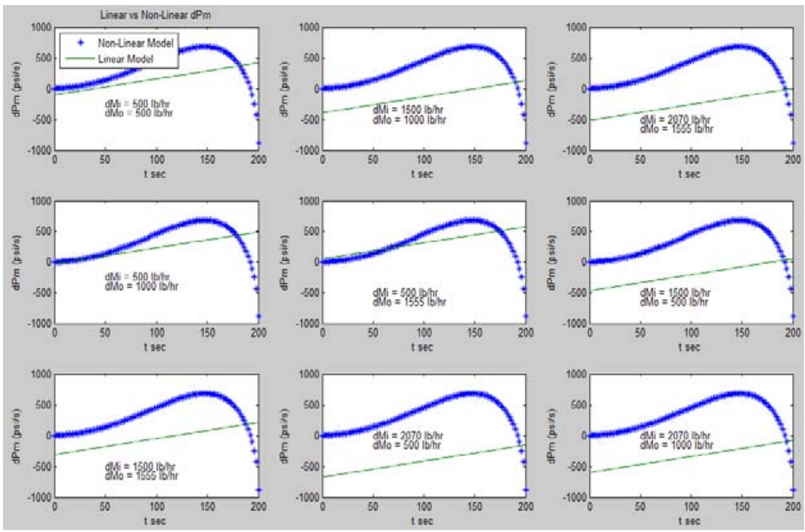
Linear vs Non-Linear dPm
Non-Linear Model
Linear Model
dMi = 500 lb/hr dMo = 500 lb/hr
dMi = 1500 lb/hr dMo = 1000 lb/hr
dMi = 2070 lb/hr dMo = 1555 lb/hr
dMi = 500 lb/hr dMo = 1000 lb/hr
dMi = 500 lb/hr dMo = 1555 lb/hr
dMi = 1500 lb/hr dMo = 500 lb/hr
dMi = 1500 lb/hr dMo = 1555 lb/hr
dMi = 2070 lb/hr dMo = 500 lb/hr
dMi = 2070 lb/hr dMo = 1000 lb/hr
dPm (psi/s)
t sec

(c)

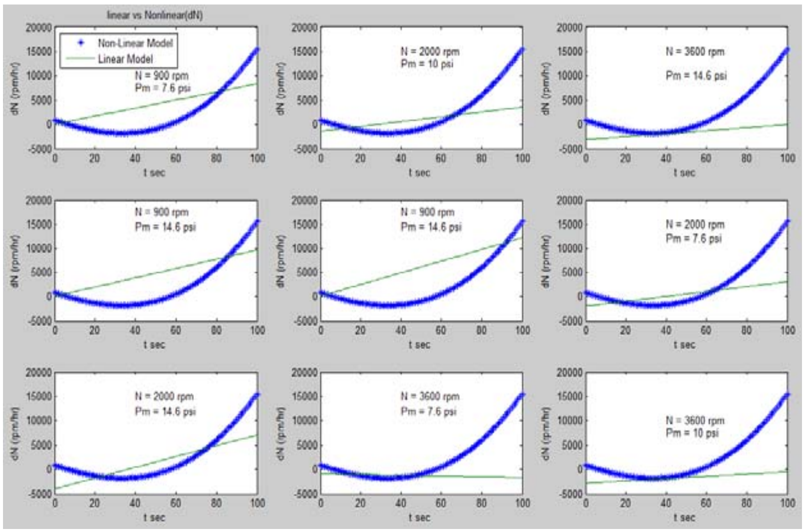

d)

Figure 3: Test results of the operating conditions combinations for (a) $\dot{M}_i$ (b) $\dot{M}_o$ (c) $\dot{P}_m$ (d) $\dot{N}$

5. CLOSED LOOP FEEDBACK CONTROL

The ability of the extended observer, with gain scheduling control, was tested in order to access its performance in a closed loop control system. Such a system was designed using a Linear Quadratic Regulator (LQR) [26] as depicted in Fig. 4. The system was designed to meet a desired output command, in this case the engine speed, and for the minimization of the cost function which is described in the following expression:

$$J(u) = \int_0^{t_f} (\hat{x}^T Q \hat{x} + u^T R u)\, dt \tag{15}$$

in which $\hat{x}$ is the observer state vector, $\hat{x}^T$ is the transpose of the observed state vector and t_f is the final time. Q is the state cost matrix and R is the performance index matrix, both are symmetric positive semi definite matrices. u and u^T are the input and corresponding transpose, respectively. The term $\hat{x}^T Q \hat{x}$ is the accumulated penalty on the state, so that it doesn't deviate much from the desired value. $u^T R u$ represents the accumulated penalty on the control input to reduce actuator effort. The closed loop system used the feedback law expressed in equation 16. It is a relationship between u and $\hat{x}$ for optimal state feedback.

$$u = -L\hat{x} \tag{16}$$

$$L = R^{-1} B^T P \tag{17}$$

$$A^T P + PA + Q - PBR^{-1} B^T P = 0 \tag{18}$$

L is the gain vector and P is the weighting factor which is the solution to the Algebraic Riccati Equation (ARE) described in equation 18.

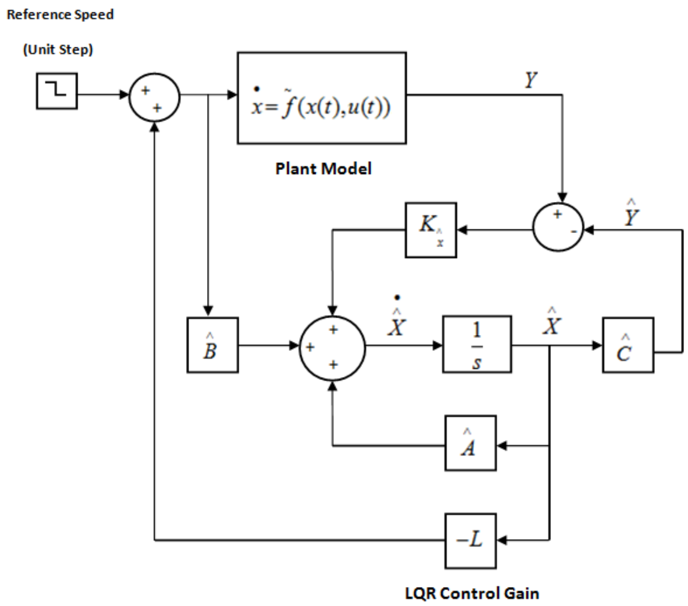

Figure 4: Block diagram representation of the closed loop control

6. SIMULATION RESULTS

Matlab was used to create the simulation of the extended observer and we applied it to the IC engine model, first as the open loop system in Fig.2. The simulated input was a step function of magnitude 20, which represents a throttle angle of 20 degrees at startup. Each state were observed and estimated and the observed nonlinear curve from the extended observer was directly compared to the nonlinear system curve in Figures 5 (a-d). Table 4 includes all the parameters used for simulation and Table 5 includes the range, operating conditions and different gains for the state-dependent gain scheduling scheme.

Table 4: Model parameters

σ	15 deg. BTDC
A/F	14.6
T_{load}	6 ft-lb
K_p	0.516
$\dot{M}_e$	6 lb/hr
P_a	14.7 psi
J_e	0.14 ft-lb-s^2

Table 5: Gain scheduling parameters: ranges, operating conditions, gains and observer poles.

Ranges	Operating Conditions	Gain $K_{\hat{x}}(t)$	
$0 < x_1 \leq 500$ lb/hr	$\theta = 22^{o}$	[-0.78 -18.8798 -2.4 -255.633]	$P_m = 7.3$ psi
$x_1 > 500$ lb/hr	$\theta = 42$	[-0.78 -3.6709 -0.4731 -47.896]	$P_m = 10$ psi
$0 < x_2 \leq 84.8$ lb/hr	$N = 900$ r	[-0.78 -6.1310 -0.6186 -59.317]	$P_m = 7.6$ psi
$84.8 < x_2 \leq 618$ lb/hr	$N = 900$	[-0.78 -6.3368 -0.6426 -44.370]	$P_m = 10$ psi
$618 < x_2 \leq 727.7$ lb/hr	$N = 2000$ rpm	[-0.78 -7.8622 -0.9359 -60.845]	$P_m = 10$ psi
$x_2 > 727.7$ lb/hr	$N = 3600$ rpm	[-0.78 -11.2251 -1.5469 -58.352]	$P_m = 14.6$ psi
$0 < x_3 \leq 49.85$ psi/h	$\dot{M}_i = 500$ lb/hr	[-0.78 -7.5039 -0.8826 -80.043]	$\dot{M}_o = 1000$ lb/hr
$x_3 < 49.85$ psi/hr	$\dot{M}_i = 500$ lb/hr	[-0.78 -7.5039 -0.8826 -80.043]	$\dot{M}_o = 1555$ lb/hr
$0 < x_4 \leq 1813$ rpm/hr	$N = 900$ rpm	[-1.56 -10.4109 -0.3157 -242.345]	$P_m = 7.6$ psi
$x_4 < 1813$ rpm/hr	$N = 2000$ rpm	[-1.34 -10.7268 -0.3707 -212.911]	$P_m = 10$ psi

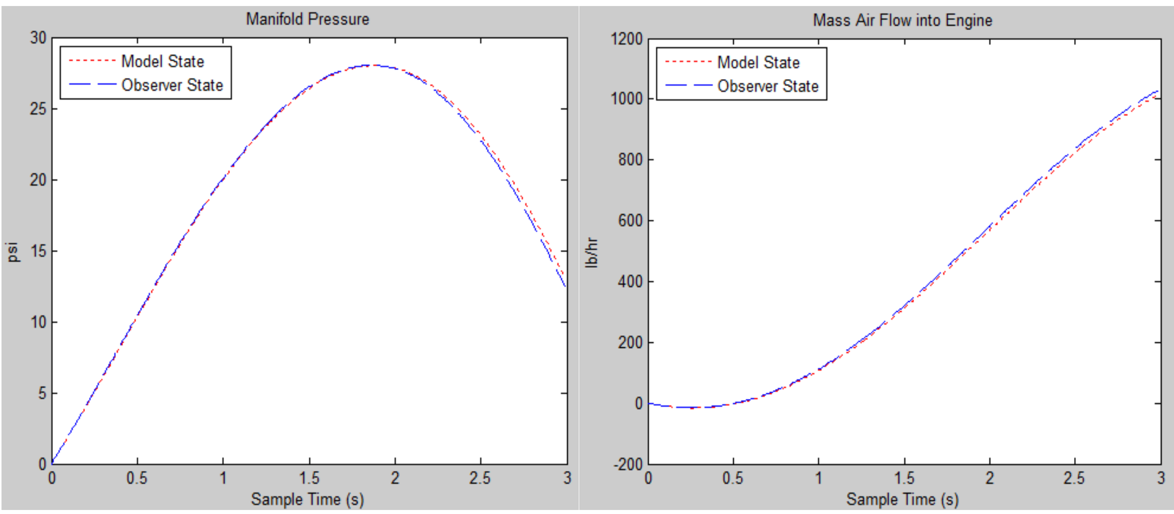

(a) (b)

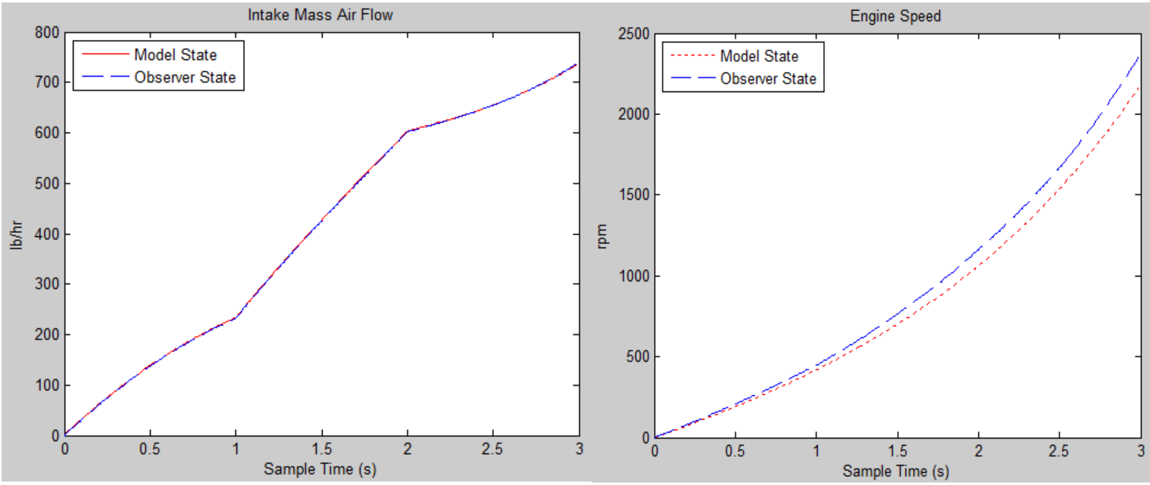

(c) (d)

Figure 5: Simulation of extended observer states estimation: (a) $\dot{M}_i$ (b) $\dot{M}_o$ (c) P_m (d) N

Figure 6 shows the output response of the LQR to a command of 2000 RPM. There is a slight 2% overshoot, and a 3% steady state error and the settling time is about 2.5 seconds. It includes the output response to a +/- 20% variation in the model parameter. The 20% increase and decrease in the model parameters did not affect the performance significantly as far as the overshoot and steady state error are concerned. The overshoot stayed within a 2.5% range and the steady state error within a 3.5% range. The most significant change came in the -20% variation settling time which increased from 2 seconds to close to 10 seconds.

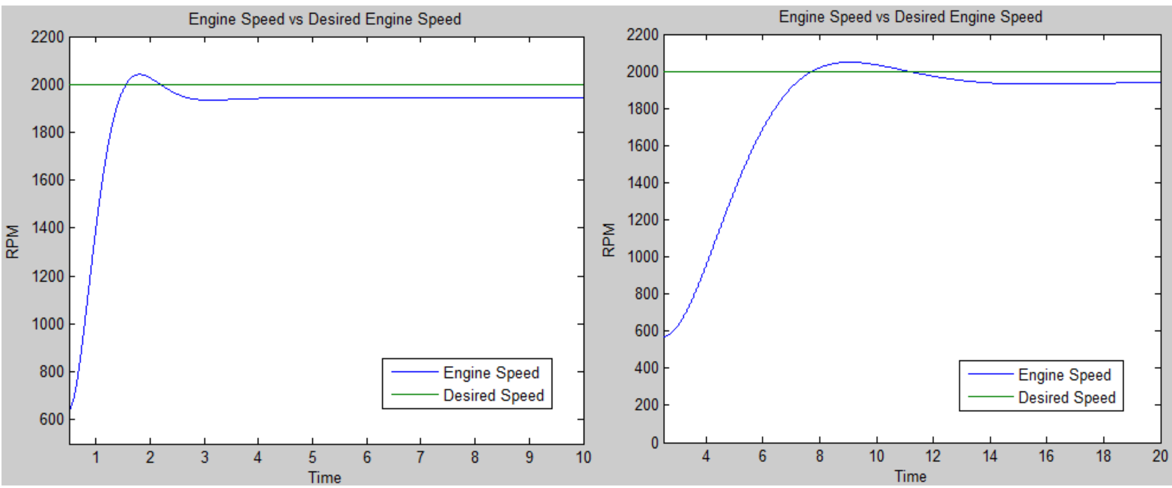

(a) (b)

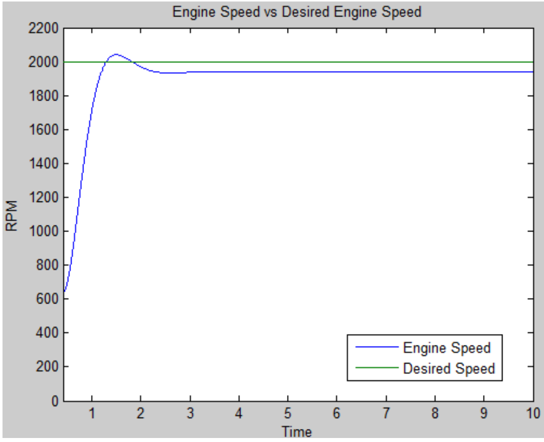

(c)

Figure 6: Output response to desired engine speed command: (a) Original system Parameters (b) -20% parameter variation (c) +20% parameter variati

T_{Load} = 10 ft-lb

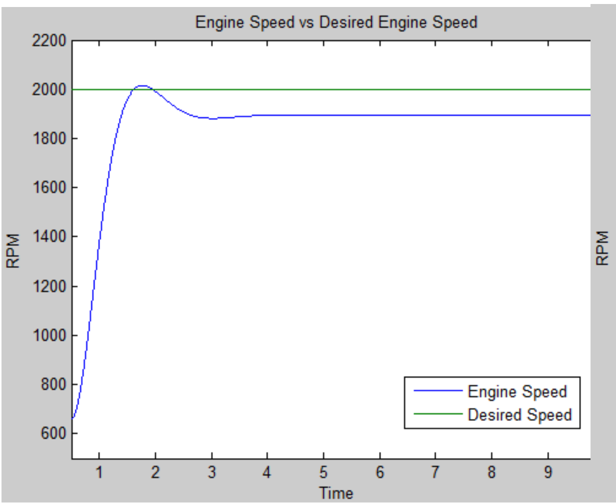

T_{LOAD}= 20 ft-lb

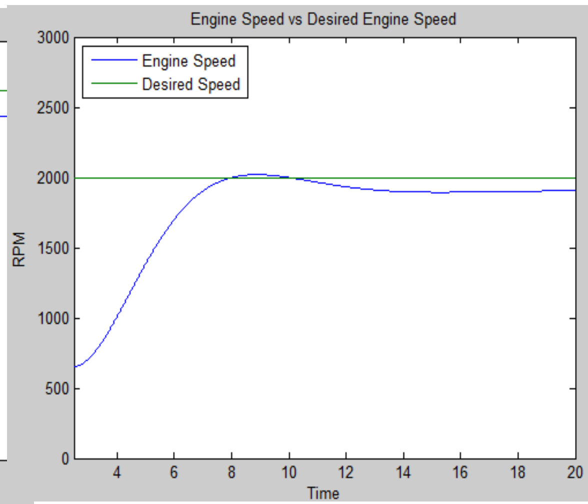

T_{Load} = 50 ft-lb

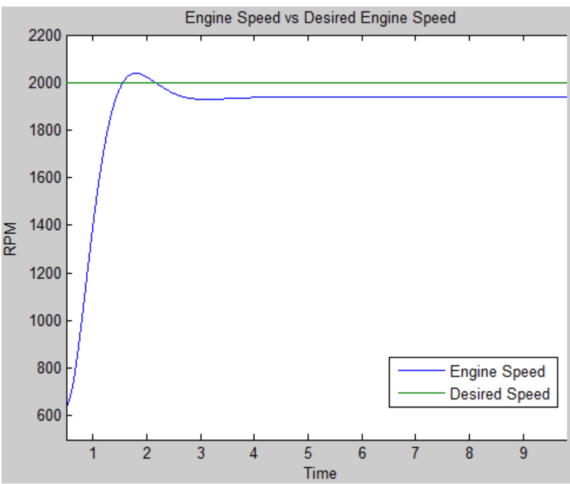

T_{Load} = 10 ft-lb, -20% parameter variation

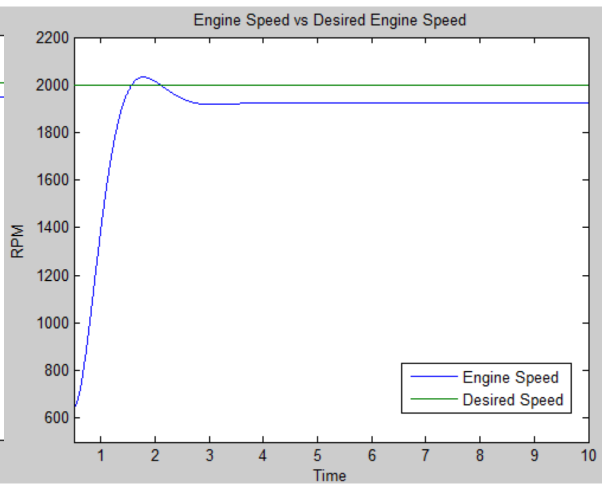

T_{Load} = 20 ft-lb, -20% parameter variation

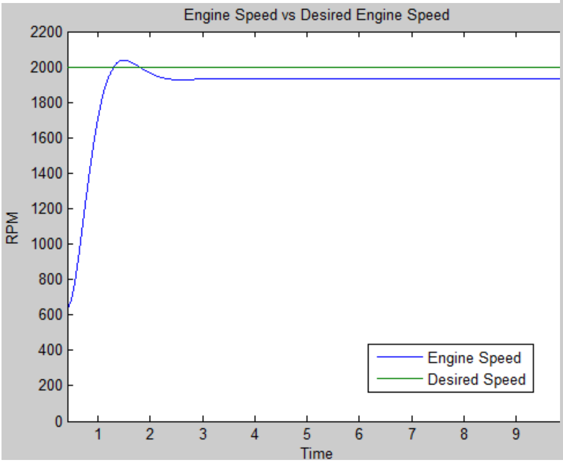

T_{Load} = 50 ft-lb, -20% parameter variation

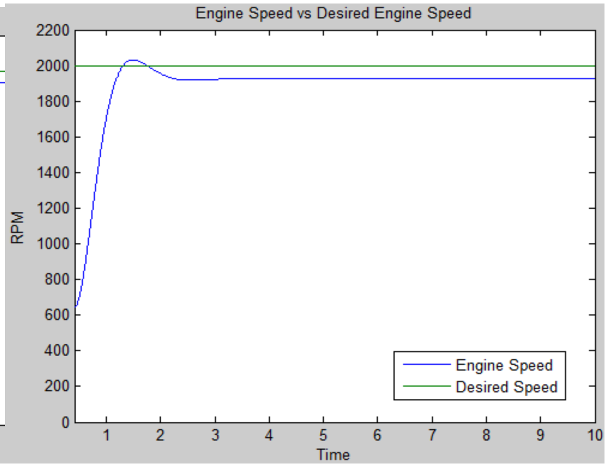

T_{Load} = 10 ft-lb, +20% parameter variation

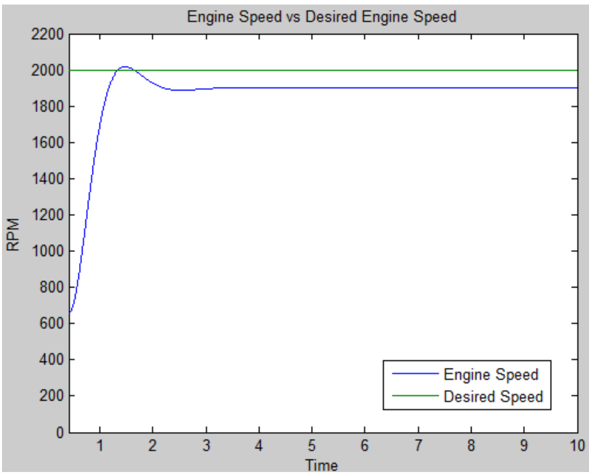

T_{Load} = 20 ft-lb, +20% parameter variation

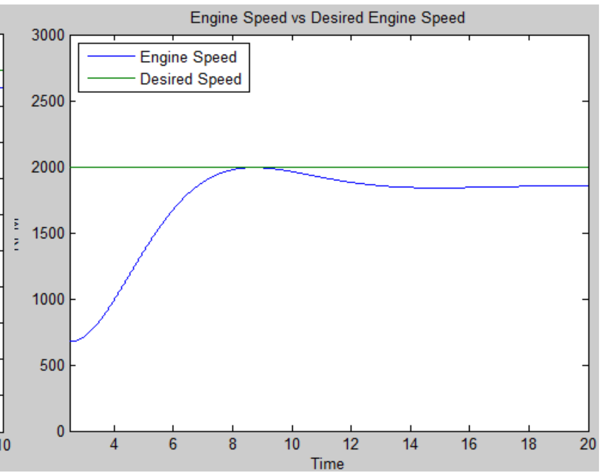

T_{Load} = 50 ft-lb, +20% parameter variation

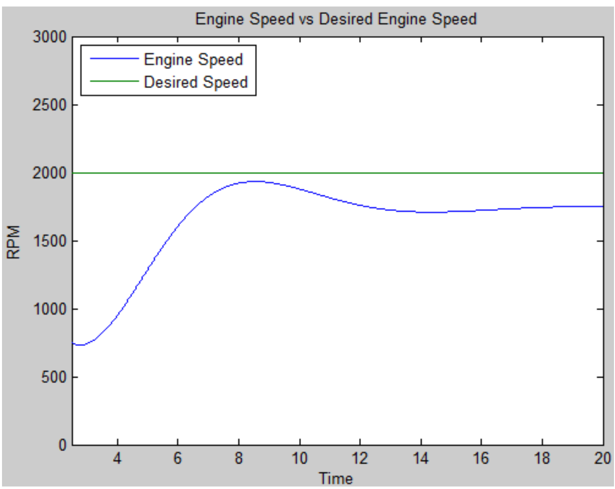

Figure 7: Output response to disturbance variations

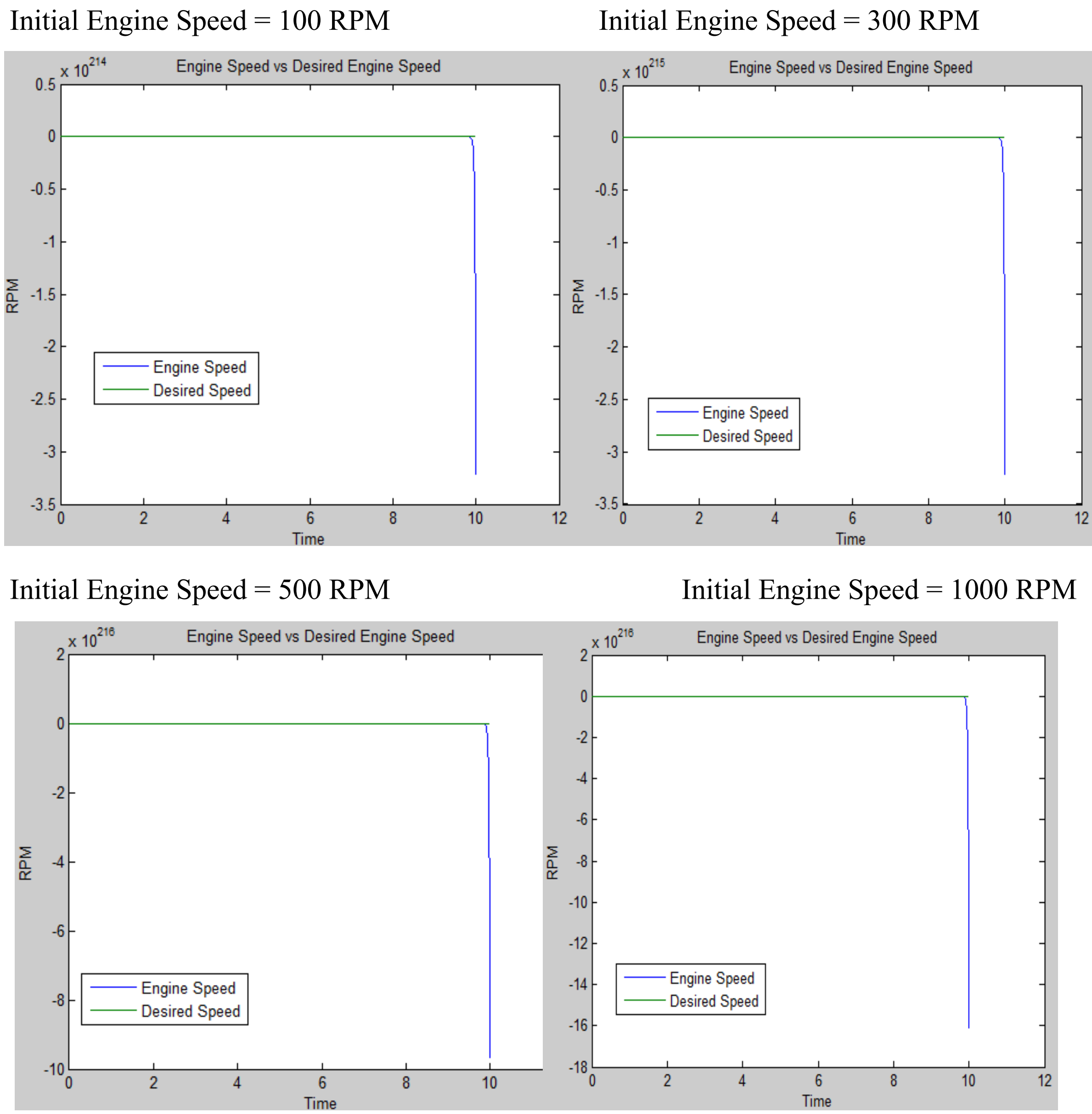

Figure 8: Output response to initial condition variations

In Figure 7, the disturbance on the system was increased by increasing the load torque in equation 8. As the disturbance increased, the overshoot decreased and the steady state error increased slightly. In other words, the LQR overcompensated so much that the desired speed would never be reached, however the error didn't exceed 5.5% under added load torque disturbance. The +/- 20% model variations exhibited similar behavior as the overshoot decreased and steady state error increased with added disturbance.

Figure 8 shows that the LQR is very sensitive to initial condition variations. The initial conditions were varied from their zero state conditions. The system exhibited instability and the magnitude of the instability grew as the initial conditions increased. This similar phenomena took place for the +/- 20% variation in the model parameters.

7. CONCLUSION

We were able to successfully implement an extended observer and apply it to a nonlinear internal combustion engine model. All parameters were chosen based on actual data aided by simulation test results. We used state-dependent gain scheduling control by changing the operating conditions depending on the current state values. The results demonstrated that the extended observer, along with a gain scheduling method can successfully and very accurately estimate the internal states of the system for feedback control. This paper can be extended to other types of engines or IC engine models, particularly more complex models. This model was simplified and only contained 4 states. But with a more complex model, component connection or other techniques could be used for order reduction. Then the extended observer and gain scheduling control could be utilized as it was in this paper. Other linearization techniques could be applied in future work, such as piecewise linear modeling.

REFERENCES

[1] D. Dobner, "A Mathematical Engine Model for Development of Dynamic Engine Control," SAE Technical Paper, 1980.

[2] A. Cook and B. K. Powell, "Modeling of an Internal Combustion Engine for Control Analysis," IEEE Control Systems Magazine, Vol. 8, Issue 4, pp. 20-26, 1988.

[3] R. Zhang, and M. Chang, "Systematic Model-Based Engine Control Design," SAE Technical Paper, 2008.

[4] N. Cavina, et al. "Model-Based Idle Speed Control for a High Performance Engine," SAE Technical Paper, 2003.

[5] J. Fiaschetti, and N. Narasimhamurthi, "A Descriptive Bibliography of SI Engine Modeling and Control," SAE Technical Paper, 1995.

[6] G. Lowe, and M. Zohdy, "Modeling Nonlinear Systems using Multiple Piecewise Linear Equations," Nonlinear Analysis: Modelling and Control, Vol. 15, Issue 4, pp. 451-458, 2010.

[7] G. Lowe and M. Zohdy, "A Technique for using H2 and H∞ Robust State Estimation on Nonlinear Systems," IEEE International Conference on Electro/Information Technology, pp. 109-115, 2009.

[8] F. Caliskan, and M. Zohdy, "Robust Quadratic Stabilization Applied to Design of Continuous-Time and Discrete-Time Observers," ISA transactions, Vol. 42, Issue 3, pp. 381-389, 2003.

[9] D. Luenberger, "An Introduction to Observers," IEEE Transactions on Automatic Control, Vol. 16, Issue 6, pp. 596-602, 1871.

[10] K. Ogata, Modern Control Engineering, Upper Saddle River, New Jersey, Prentice Hall, 2010.

[11] T. Kailath, Linear Systems, Upper Saddle River, New Jersey, Prentice Hall, 1980.

[12] T.Du, P. Vas, and F. Stronach, "Design and Application of Extended Observers for Joint State and Parameter Estimation in High-Performance AC Drives," Electric Power Applications, IEE Proceedings, Vol. 142, Issue 2, pp. 71-78, 1995.

[13] L. Imsland, et al. "Nonlinear Observer for Vehicle Velocity with Friction and Road Bank Angle Adaptation - Validation and Comparison with an Extended Kalman Filter," SAE Technical Paper, 2008.
[14] Q. Zheng, "On the Validation of Extended State Observer through Analysis and Experimentation," Journal of Dynamic Systems, Measurement, and Control, Vol. 134, 2012.
[15] V. Kaparin, and U. Kotta, "Extended Observer Form for Discrete-Time Nonlinear Control Systems," 9th IEEE International Conference on Control and Automation (ICCA), pp. 507-512, 2011.
[16] Lee, B., Y. Guezennec, and G. Rizzoni, "Model-Based Fault Diagnosis of Spark-Ignition Direct-Injection Engine using Nonlinear Estimations," SAE Technical Paper, 2005.
[17] Y. Wang, and F. Chu, "Application of Nonlinear Observer to On-line Estimation of Indicated Torque in Automotive Engines," Department of Precision Instruments and Mechanology, Tsinghua University, Beijing, 2005.
[18] W.E. Leitheadand D. J. Leith, "Survey of Gain-Scheduling Analysis and Design," International Journal of Control, Vol. 73, Issue 11, pp. 1001-1025, 2000.
[19] B. K. Powell, "A Dynamic Model for Automotive Engine Control Analysis," 18th IEEE Conference on Decision and Control including the Symposium on Adaptive Processes, pp. 120-126, 1979.
[20] K.H. Khalil, Nonlinear Systems, 3rd. ed. Upper Saddle River, New Jersey, Prentice Hall, 2002.
[21] A. Kwiatkowski et al., "Application of LPV Gain Scheduling to Charge Control of a SI Engine," IEEE International Symposium on Intelligent Control, pp. 2327-2331, 2006.
[22] Nohra et al., "A Nonlinear Approach with Gain Schedule Control Adaptation for a Complete-Model Diesel-Engine Diagnosis," 3rd International Symposium on Communications, Control and Signal Processing ISCCSP, pp. 689-696, 2008.
[23] F. Syed et al., "Rule-Based Fuzzy Gain-Scheduling PI Controller to Improve Engine Speed and Power Behavior in a Power-Split Hybrid Electric Vehicle," Fuzzy Information Processing Society (NAFIPS), pp. 284-289, 2006.
[24] F. Syed et al., "Fuzzy Gain-Scheduling Proportional–Integral Control for Improving Engine Power and Speed Behavior in a Hybrid Electric Vehicle," IEEE Transactions on Vehicular Technology, Vol. 58, Issue 1, pp. 69-84, 2009.
[25] W. Xiukun and L. del Re, "Gain Scheduled Control for Air Path Systems of Diesel Engines using LPV Techniques," IEEE Transactions on Control Systems Technology, Vol. 15, Issue 3, pp. 406-15, 2007.
[26] P. Dorato, C. Abdallah, and V. Cerone, "Linear-Quadratic Control, an Introduction," Englewood Cliffs, New Jersey: Prentice Hall, 1995.